data are available from second-rotation plantations, these effects would likely be exacerbated after harvesting, owing to the export of cations and other nutrients off site. In the framework described above, the potential positive and negative benefits of plantations for salinity are predictable based on the presence and type of groundwater available, biophysical evaporative demand, and soil texture.

Plantations provide a proven tool for managing Earth's carbon cycle. The Clean Development Mechanism of the Kyoto Protocol allows countries to offset part of their CO_2 emissions through carbon sequestration, when consistent with a country's sustainable development objectives. New carbon trading exchanges such as the European Union's Greenhouse Gas Emission Trading Scheme help make such offsets a reality. As demand increases for land to accommodate plantations, more comprehensive environmental planning will be needed to avoid problems and to manage land successfully and sustainably. One way to do this is to compare the value of other ecosystem services gained or lost with those of carbon sequestration. The field of ecosystem services valuation is becoming increasingly sophisticated, and markets are opening up for some other services. The co-benefits and trade-offs of plantations need to be taken into account when negotiating exchange agreements. We believe that decreased stream flow and changes in soil and water quality are likely as plantations are increasingly grown for biological carbon sequestration.

References and Notes

1. P. M. Vitousek, *J. Environ. Qual.* **20**, 348 (1991).
2. R. A. Houghton, J. L. Hackler, K. T. Lawrence, *Science* **285**, 574 (1999).
3. M. I. Hoffert *et al.*, *Science* **298**, 981 (2002).
4. R. B. Jackson, J. L. Banner, E. G. Jobbágy, W. T. Pockman, D. H. Wall, *Nature* **418**, 623 (2002).
5. S. Pacala, R. Socolow, *Science* **305**, 968 (2004).
6. R. B. Jackson, W. H. Schlesinger, *Proc. Natl. Acad. Sci. U.S.A.* **101**, 15827 (2004).
7. B. A. McCarl, U. A. Schneider, *Science* **294**, 2481 (2001).
8. J. A. Wright, A. DiNicola, E. Gaitan, *J. Forestry* **98**, 20 (2000).
9. A. J. Pearce, L. K. Rowe, *J. Hydrol. N.Z.* **18**, 73 (1979).
10. L. Zhang, W. R. Dawes, G. R. Walker, *Water Resour. Res.* **37**, 701 (2001).
11. M. G. R. Cannell, *New For.* **17**, 239 (1999).
12. K. A. Farley, E. G. Jobbágy, R. B. Jackson, *Glob. Change Biol.* **11**, 1565 (2005).
13. Materials and methods and supporting material are available on *Science* Online.
14. Y. Xue, M. J. Fennessy, P. J. Sellers, *J. Geophys. Res.* **101**, 7419 (1996).
15. R. A. Pielke, R. Avissar, *Landscape Ecol.* **4**, 133 (1990).
16. S. Baidya Roy, R. Avissar, *J. Geophys. Res.* **107**, (D20), 8037 (2002).
17. W. A. Hoffmann, R. B. Jackson, *J. Clim.* **13**, 1593 (2000).
18. D. M. Adams, R. J. Alig, J. M. Callaway, B. A. McCarl, S. M. Winnett, "The forest and agriculture sector optimization model (FASOM): Model structure and policy applications" (Research Paper PNW-RP-495, USDA Forest Service, Pacific Northwest Research Station, Portland, Oregon, 1996).
19. W. R. Cotton *et al.*, *Meteor. Atmos. Phys* **82**, 5 (2003).
20. R. E. Dickinson, P. Kennedy, *Geophys. Res. Lett.* **19**, 1947 (1992).
21. D. C. Le Maitre, D. F. Scott, C. Colvin, *Water S.A.* **25**, 137 (1999).
22. E. G. Jobbágy, R. B. Jackson, *Glob. Change Biol.* **10**, 1299 (2004).
23. A. Heuperman, *Agric. Water Manage.* **39**, 153 (1999).
24. M. K. Sapanov, *Eurasian Soil Sci.* **33**, 1157 (2000).
25. G. R. Walker, L. Zhang, T. W. Ellis, T. J. Hatton, C. Petheram, *Hydrogeol. J.* **10**, 68 (2002).
26. S. K. Pattanayak *et al.*, *Clim. Change* **71**, 341 (2005).
27. R. J. George *et al.*, *Agric. Water Manage.* **39**, 91 (1999).
28. A. J. Plantinga, J. Wu, *Land Econ.* **79**, 74 (2003).
29. D. F. Scott, W. Lesch, *J. Hydrol.* **199**, 360 (1997).

30. We gratefully acknowledge the Duke University Center on Global Change and Provost's Office, the U.S. National Science Foundation, the National Institute for Global Environmental Change of the U.S. Department of Energy, the Inter-American Institute for Global Change Research, the Andrew W. Mellon Foundation, and the CSIR for financial support. A. Mendoza assisted with the database, and W. H. Schlesinger and two anonymous reviewers provided helpful suggestions on the manuscript.

Supporting Online Material

www.sciencemag.org/cgi/content/full/310/5756/1944/DC1
Materials and Methods
Tables S1 to S3
References

24 August 2005; accepted 21 November 2005
10.1126/science.1119282

Heterogeneous Hadean Hafnium: Evidence of Continental Crust at 4.4 to 4.5 Ga

T. M. Harrison,[1,2]* J. Blichert-Toft,[3] W. Müller,[1,4] F. Albarede,[3] P. Holden,[1] S. J. Mojzsis[5]

The long-favored paradigm for the development of continental crust is one of progressive growth beginning at ~4 billion years ago (Ga). To test this hypothesis, we measured initial $^{176}Hf/^{177}Hf$ values of 4.01- to 4.37-Ga detrital zircons from Jack Hills, Western Australia. ε_{Hf} (deviations of $^{176}Hf/^{177}Hf$ from bulk Earth in parts per 10^4) values show large positive and negative deviations from those of the bulk Earth. Negative values indicate the development of a Lu/Hf reservoir that is consistent with the formation of continental crust (Lu/Hf ≈ 0.01), perhaps as early as 4.5 Ga. Positive ε_{Hf} deviations require early and likely widespread depletion of the upper mantle. These results support the view that continental crust had formed by 4.4 to 4.5 Ga and was rapidly recycled into the mantle.

A fundamental question of Earth's evolution is: When did the growth of continental crust begin? One model is that the first crust formed after 4 Ga and grew slowly until the present day (*1*, *2*). This view reflects the absence of a >4-Ga rock record (*3*) and the broadly coherent post–4 Ga evolution of depleted mantle $^{143}Nd/^{144}Nd$ (*4*) and $^{176}Hf/^{177}Hf$ (*5*). Long-standing observations of early Nd (*6*) and Hf (*7*, *8*) depletions, however, leave open the possibility of even earlier global fractionations. Another view (*9*, *10*) is that continental crust was widespread during the Hadean Eon [the first 500 million years (My) of Earth history]. In such a scenario, the lack of direct evidence of earlier depletion events reflects subsequent remixing. Detrital zircons from Jack Hills, Western Australia, with 4.0- to 4.4-Ga U-Pb ages (*11*–*13*) represent pieces of crust that have been sequestered for up to ~4.4 Ga. Hf isotopic compositions vary because of radioactive decay of ^{176}Lu, and such variations in zircons constitute an excellent tracer of Earth's crust/mantle differentiation. This is because zircons have very low Lu/Hf ratios and thus record near-initial $^{176}Hf/^{177}Hf$ at the time given by their U-Pb age. Amelin and co-workers (*14*) investigated Hf isotopes in Jack Hills zircons as old as 4.14 Ga and inferred the existence of reworked Hadean crust. We have now extended this application by undertaking Lu-Hf analyses of grains ranging in age up to 4.37 Ga, thereby narrowing the gap to less than 200 My from the end of Earth's accretion to the first mineral record. We document significant Hf isotopic heterogeneity during the early Hadean and conclude that major differentiation of the silicate Earth, possibly the formation of continental crust with a volume similar in magnitude to the present day, may have occurred by 4.4 to 4.5 Ga.

Using the multicollector Sensitive High Resolution Ion Microprobe II, we have surveyed the radiogenic $^{207}Pb/^{206}Pb$ ($^{207}Pb/^{206}Pb^*$) ratio

[1]Research School of Earth Sciences, Australian National University, Canberra, ACT 0200, Australia. [2]Department of Earth and Space Sciences and Institute of Geophysics and Planetary Physics, University of California at Los Angeles, Los Angeles, CA 90095, USA. [3]Ecole Normale Supérieure, CNRS Unité Mixte de Recherche 5570, 69364 Lyon Cedex 7, France. [4]Department of Geology, Royal Holloway University of London, Egham, TW20 0EX, UK. [5]Department of Geological Sciences, University of Colorado, Boulder, CO 80309, USA.

*To whom correspondence should be addressed. E-mail: mark.harrison@anu.edu.au

of over 50,000 Jack Hills zircons separated from a large conglomerate sample (JH992) obtained from the original locality of Compston and Pidgeon (*11*). Hadean grains thus identified were dated by the U-Pb method (*11–13*). Zircons between 4.01 and 4.37 Ga were then analyzed for Lu/Hf and Hf isotopic composition (tables S1 and S2). Although $^{207}Pb/^{206}Pb^*$ ages can be variable within Hadean zircons (*11–13*), it is rarely the case (*15*) that an individual grain exhibits more than two generations of crystal growth. In the cases of concordant or nearly concordant (<12% discordant) results, we assume that the $^{207}Pb/^{206}Pb^*$ age records the time of crystallization, which we then use to calculate $\varepsilon_{Hf(T)}$, where T is age. For grains that showed evidence of zoning or yielded apparent $\varepsilon_{Hf(T)}$ values that strongly deviated from those of bulk Earth, we undertook additional ion microprobe dating investigations to assess whether multiple generations of zircon growth were present (table S2 and fig. S2).

Of the 104 multicollector–inductively coupled plasma–mass spectrometry (MC-ICP-MS) zircon $^{176}Hf/^{177}Hf$ results we present, 44 were measured by solution MC-ICP-MS (table S1) (*16*) and 60 by laser ablation MC-ICP-MS (table S2) (*16*). We deliberately used both approaches, because each has potential limitations that are in part compensated for by the other. Solution MC-ICP-MS provides a bulk Hf isotope composition, but does not suffer from isobaric interferences on ^{176}Hf from Yb and Lu. Although laser ablation MC-ICP-MS measurements require peak stripping to correct for Yb and Lu interferences on ^{176}Hf, they allow spatially resolved analysis using spots of 60 to 80 μm in diameter, which facilitates the identification of zircons zoned with respect to $^{176}Hf/^{177}Hf$. Because these analyses retain some of the zircon under analysis, subsequent ion microprobe investigations of potential age heterogeneity are possible.

We calculated $\varepsilon_{Hf(T)}$ using the "terrestrial" ^{176}Lu decay constant (λ_{176}) of $1.867 \pm 0.008 \times 10^{-11}$ year^{-1} [(*17*) and references therein] and the present day chondritic parameters $^{176}Lu/^{177}Hf = 0.0332 \pm 0.0002$ and $^{176}Hf/^{177}Hf = 0.282772 \pm 29$ (*18*) [λ_{176} and solar system initial $^{176}Hf/^{177}Hf$ deduced from meteorite Lu-Hf isochrons appear to reflect irradiation effects in the solar nebula (*19*)]. Using the chondritic averages of Patchett and co-workers (*20*) instead would not significantly change our calculated values of $\varepsilon_{Hf(T)}$, because their $^{176}Hf/^{177}Hf$ and Lu/Hf values all fall on the same 4.5-Ga isochron as those in (*18*).

Our data (tables S1 and S2) show a high degree of Hf isotope heterogeneity, with variation in $\varepsilon_{Hf(T)}$ values at 4.2 Ga of over 20 ε units. Before we examine the geological significance of these data, we investigate possible artifacts of combined interpretation of Lu-Hf and U-Pb systematics in a complex zircon population that could lead to incorrect inferences of early deviations from chondritic evolution. A key link in using zircon to assess initial Hf isotopic ratios is that the age ascribed accurately reflects the time at which the Hf isotopic composition was incorporated into the zircon. In the case of a zircon zoned in U-Pb age, relating an older age component to the bulk Hf isotope composition could result in an incorrect estimate of $\varepsilon_{Hf(T)}$.

For example, consider the case of grain CU05 8.5, which yields an ion microprobe age of 4123 ± 18 Ma and age-corrected solution MC-ICP-MS $^{176}Hf/^{177}Hf = 0.280415 \pm 0.000015$ (2 SE) (table S1), corresponding to an apparent $\varepsilon_{Hf(T)} = +10.7 \pm 0.5$. However, because the bulk solution ICP-MS $^{207}Pb/^{206}Pb$ age is only 3624 Ma (*21*), we infer that this grain is substantially heterogeneous with respect to age and that the ~4.1-Ga ion microprobe date represents only a small portion of the total U-Pb system. If we instead use the bulk 3.62-Ga age, the apparent ε_{Hf} drops to a near–bulk Earth value of $+1.2 \pm 0.5$. We thus eliminated this sample from further consideration.

Less obvious is that mixtures of concordant components with contrasting U concentrations each plotting on bulk Earth could also yield substantial positive and negative deviations in ε_{Hf}. This is because of the strongly nonlinear relationship between $^{207}Pb/^{206}Pb^*$ (or Pb/U) and age, whereas the long half-life of ^{176}Lu resulted in essentially linear growth in $^{176}Hf/^{177}Hf$ over the past 4.56 Gy. To assess this effect, we developed a model in which concordant core (T1) and rim (T2) ages are characterized by $\varepsilon_{Hf(T)}$ at T1 and T2, respectively. If the bulk age of this composite is characterized by a U-Pb date obtained by ion microprobe spot analysis in the core, but associated with a $^{176}Hf/^{177}Hf$ ratio that is a mixture of the two end-members, an incorrect value of ε_{Hf} results. Even in the case for which U-Pb age and Hf isotopes are measured on the same spot overlapping these two zones, aberrant values can result. Figure 1 illustrates possible trajectories in $\varepsilon_{Hf(T)}$ resulting from mixing two such components. Because variations in U concentration are far greater than those in Hf concentration (*22*), we only varied U concentrations.

Consider the case of a 4.4-Ga core ($^{176}Hf/^{177}Hf_{4.4\ Ga} = 0.279930$) and a 3.7-Ga rim ($^{176}Hf/^{177}Hf_{3.7\ Ga} = 0.280398$) (i.e., an age contrast of 1 half-life of ^{235}U). Mixtures of these two components between 0 and 100%, shown in 10% increments, are indicated by the black symbols (Fig. 1). The variation in symbol shape represents differing U concentrations of the 4.4-Ga core (T1) and the 3.7-Ga rim (T2). For the case of equal U concentration (diamonds), mixing produces a roughly symmetric trajectory in positive ε_{Hf} space, reaching an ε_{Hf} value of +2 at ~4 Ga. Doubling the U concentration in the core relative to the rim (squares) increases the apparent ε_{Hf} value to close to +5. This is expected because the Hf isotope composition at every intermediate position is associated with an older apparent $^{207}Pb/^{206}Pb^*$ age and thus appears to originate in a higher Lu/Hf environment. Where the rim U concentration is a factor of 1.6 greater than in the core (circles), no variation from bulk Earth is seen (because $^{207}Pb/^{206}Pb^*$ drops by a factor of 1.6 for each half-life of ^{235}U). Thus, the reduced rate of generation of Pb* at 3.7 Ga is in this case exactly offset by the 160% greater U content of the rim. Where U in the core is 10 times less than in the rim (triangles), ε_{Hf} values as negative as –7 result.

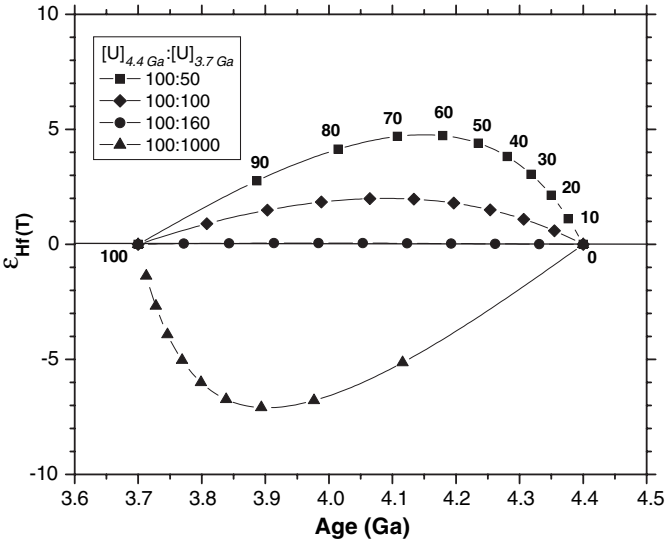

Fig. 1. Results of a model illustrating possible trajectories in $\varepsilon_{Hf(T)}$ versus age space ensuing from mixing zircon components of differing age, U concentration, and Hf isotope composition. The model assumes concordant ages of T1 (core) and T2 (rim), which are characterized by the Hf isotope composition of bulk Earth at T1 and T2, respectively. Mixtures of the two components are shown adjacent the relevant curve in % of the rim component for the case of a 4.4-Ga core and 3.7-Ga rim. Where the bulk age of a mixture is characterized by a U-Pb age in the core, but incorrectly associated with a $^{176}Hf/^{177}Hf$ ratio that is a mixture of the two end-members, the potential exists for incorrect ε_{Hf} values to be calculated. More surprising is that in the case where U-Pb age and Hf isotopes are measured on the same spot overlapping these two zones, aberrant values result, as shown in the mixing curves.

For many grains analyzed by laser ablation MC-ICP-MS, further age investigations are possible, because the method is not completely destructive, compared with solution chemistry. Grains with calculated ε_{Hf} that differ from bulk Earth by more than 5 ε units were, where sufficient sample remained, redated near their rims to assess age homogeneity. In the majority of cases, $^{207}Pb/^{206}Pb$* ages were reproduced at a satisfactory level (table S2). In one case (RSES17 2.9), we were able to resolve a time-dependent $^{176}Hf/^{177}Hf$ signal that dropped by 4 ε units upon penetrating a 3469 ± 12–Ma rim from a 4127 ± 64–Ma core, yielding $\varepsilon_{Hf(4.13\ Ga)} = 10 \pm 1.3$ (table S2 and fig. S1).

Where rims are demonstrably younger than core ages, we were able to rule out mixing between domains by the lack of a time-resolved variation in the $^{176}Hf/^{177}Hf$ signal and by visual evidence from imaging studies. Even where mixing may have occurred below our ability to resolve time variations in $^{176}Hf/^{177}Hf$, we have ruled out this effect as a cause for overestimating variations in $\varepsilon_{Hf(T)}$ from bulk Earth by using our mixing model (table S2, comments). For example, grain ANU39 15.15 yields a $^{207}Pb/^{206}Pb$ age of 4234 ± 10 Ma (0% discordant), which corresponds to a high apparent $\varepsilon_{Hf(T)}$ of 15.3 ± 1.8 (table S2 and fig. S2). Both the ion microprobe spot for the U-Pb age and the laser ablation pit for the Hf isotope analysis were obtained from the central portion of the grain, which was imaged as a homogenous core (fig. S2). Although the overgrowth region was later found to yield an age of 3548 ± 10 Ma (table S2 and fig. S2), our modeling shows that the relationship between U concentrations in the core [82 parts per million (ppm)] and rim (440 ppm) would likely increase the estimated value of ε_{Hf} if a portion of the rim had inadvertently been included in the analysis. Thus, the value of ~+15 is a minimum estimate of the true ε_{Hf} of the grain core.

In four cases, measured $^{174}Hf/^{177}Hf$ and $^{178}Hf/^{177}Hf$ were outside accepted values (*16*), and these data were eliminated from consideration. Figure 2 shows the results for which we are confident that all the aforementioned effects have not affected the true ε_{Hf} values. Concordant or near-concordant results are shown as solid symbols, whereas >12% discordant results are shown as open symbols. The diagonal line extending into the negative ε_{Hf} field from an age of 4.5 Ga, labeled Lu/Hf = 0, demarcates the "forbidden region," corresponding to Lu/Hf < 0. Data plotting near this line must have been derived from an environment in which Lu was essentially completely fractionated from Hf shortly after Earth formation. If that event was the formation of continental crust, then the average continental crust $^{176}Lu/^{177}Hf$ value of ~0.01 (*23*) is a more appropriate comparator. The many results that plot along this line require formation of an enriched reservoir by 4.4 to 4.5 Ga.

Positive $\varepsilon_{Hf(T)}$ deviations observed in the same age interval have not previously been documented (*14*) and imply derivation from reservoirs with high Lu/Hf ratios. These data almost surely reflect the rapid development of depleted mantle with single-stage $^{176}Lu/^{177}Hf$ ratios within the possible range of values (0.05 and 0.2) for rocks residual from mantle melting (*24*). Whereas the depleted signature we observe is roughly symmetrical with the enriched reservoir (Fig. 2), negative ε_{Hf} values outnumber positive ε_{Hf} by 2.5:1. This is in part expected, because rocks originating from a source with a depleted signature are less petrogenetically suited to crystallizing zircon.

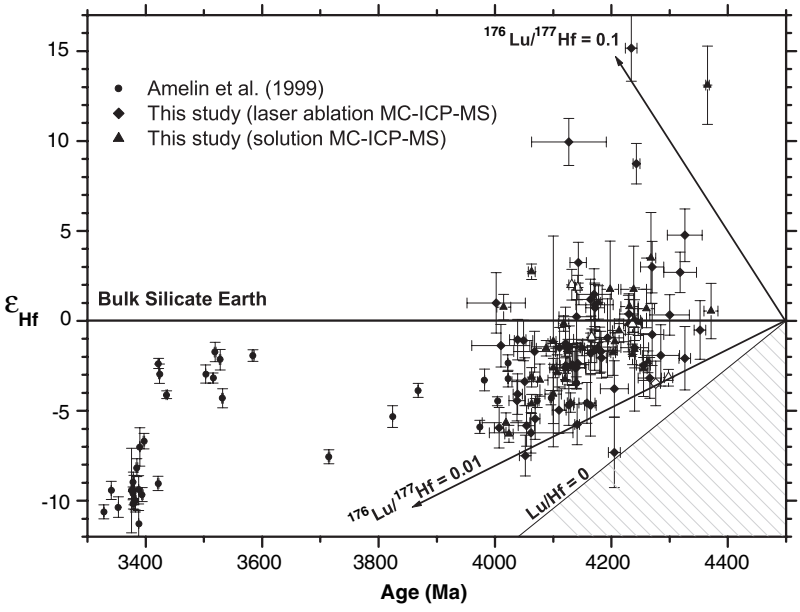

Fig. 2. Plot of $\varepsilon_{Hf(T)}$ versus age for new MC-ICP-MS Hf isotope analyses together with results of Amelin and co-workers (*14*) recalculated using the "terrestrial" ^{176}Lu decay constant (*17*). Solid symbols are concordant to <12% discordant, whereas open symbols are >12% discordant. The line marked Lu/Hf = 0 corresponds to $^{176}Hf/^{177}Hf$ ratios equivalent to the bulk silicate Earth value at 4.5 Ga. The stippled region indicates values not attainable (i.e., lower than solar system initial $^{176}Hf/^{177}Hf$). Error bars indicate 2 SE.

Most models for the growth of continental crust have emphasized delayed, slow growth (*1*, *2*, *4*). The existence of Hadean Jack Hills zircons has been known for 20 years (*11*) but has been largely considered as a curiosity rather than a fundamental record of the origin of continental crust (*25*). Investigations of Jack Hills zircons [$\delta^{18}O$, inclusion assemblages, zircon thermometry (*12*, *13*, *26*–*28*)] indicate that the vast majority formed in a continental environment (*26*) characterized by two forms of convergent margin magmatism (crustal anatexis and calc-alkaline magmatism at or close to water saturation) throughout the Hadean. Together, these data indicate that Earth was experiencing continental crust formation during the Hadean and that a mature sediment recycling system similar to that of the known era of plate tectonics had developed by ~4.4 Ga.

Jack Hills zircons are largely of continental origin (*12*, *13*, *26*–*28*), and our preferred interpretation of the variation of $\varepsilon_{Hf(T)}$ (Fig. 2) is that a major differentiation event occurred at 4.4 to 4.5 Ga, producing continental crust and a complementary depleted mantle reservoir. Because the production of modern continental crust is intimately connected with orogenic magmas, our interpretation implies that plate boundary interactions may have begun within the first ~100 My of Earth history. If the relative fraction of depleted versus enriched samples (Fig. 2) is representative of the general ongoing process, the volume of depleted mantle must have been a substantial fraction of the silicate Earth.

Positive $\varepsilon_{Hf(T)}$ deviations of +15 at ~4.2 Ga imply a reservoir with Lu/Hf of ~0.1 (Fig. 2). This extrapolates to ε_{Hf} of over +200 today, whereas values as negative as –7 at 4.2 Ga project to $\varepsilon_{Hf(0)}$ of about –100. No evidence for these reservoirs has yet been recognized in the post-Hadean rock record (*5*, *29*). Although it is conceivable that such reservoirs exist but have remained hidden for 4 Gy (*30*), their disappearance is well explained by the recycling of continental crust during the Hadean at rates ~10 times greater than those at present (*9*, *31*), coupled with vigorous stirring in a hotter and thus less-viscous mantle.

Armstrong (*9*) emphasized that all large terrestrial planets, including Earth, must have immediately differentiated into relatively constant volume core, depleted mantle, enriched crust, and fluid reservoirs. Recent investigations of $^{142,143}Nd/^{144}Nd$ variations indicate that a major silicate differentiation event occurred within 50 to 150 My (*32*, *33*), and possibly even

within 30 My (*30*) of Earth's formation. Our results support the view that continental crust was at least a component of the enriched counterpart that formed at ~4.5 Ga, but this original crust was largely recycled back into the mantle by the onset of the Archean (<4 Ga).

References and Notes

1. J. Veizer, S. L. Jansen, *J. Geol.* **87**, 341 (1979).
2. S. R. Taylor, S. M. McLennan, *The Continental Crust: Its Composition and Evolution* (Blackwell Scientific, Oxford, 1985).
3. S. A. Bowring, I. Williams, *Contrib. Mineral. Petrol.* **134**, 3 (1999).
4. M. T. McCulloch, V. C. Bennett, *Lithos* **30**, 237 (1993).
5. J. D. Vervoort, J. Blichert-Toft, *Geochim. Cosmochim. Acta* **63**, 533 (1999).
6. C. G. Chase, P. J. Patchett, *Earth Planet. Sci. Lett.* **91**, 66 (1988).
7. J. Blichert-Toft, N. T. Arndt, *Earth Planet. Sci. Lett.* **171**, 439 (1999).
8. J. Blichert-Toft, N. T. Arndt, G. Gruau, *Chem. Geol.* **207**, 261 (2004).
9. R. L. Armstrong, *Philos. Trans. R. Soc. London Ser. A* **301**, 443 (1981).
10. R. L. Armstrong, *Aust. J. Earth Sci.* **38**, 613 (1991).
11. W. Compston, R. T. Pidgeon, *Nature* **321**, 766 (1986).
12. S. J. Mojzsis, T. M. Harrison, R. T. Pidgeon, *Nature* **409**, 178 (2001).
13. S. A. Wilde, J. W. Valley, W. H. Peck, C. M. Graham, *Nature* **409**, 175 (2001).
14. Y. Amelin, D. C. Lee, A. N. Halliday, R. T. Pidgeon, *Nature* **399**, 252 (1999).
15. J. Hermann, R. Rubatto, *J. Metamorphic Geol.* **21**, 833 (2003).
16. Materials and methods are available as supporting material on *Science* Online.
17. U. Soderlund, P. J. Patchett, J. D. Vervoort, C. E. Isachsen, *Earth Planet. Sci. Lett.* **219**, 311 (2004).
18. J. Blichert-Toft, F. Albarède, *Earth Planet. Sci. Lett.* **148**, 243 (1997).
19. F. Albarède *et al.*, *Geochim. Cosmochim. Acta,* in press.
20. P. J. Patchett, J. D. Vervoort, U. Soderlund, V. J. M. Salters, *Earth Planet. Sci. Lett.* **222**, 29 (2004).
21. J. Blichert-Toft, unpublished data.
22. P. W. O. Hoskin, U. Schaltegger, *Rev. Mineral. Geochem.* **53**, 27 (2003).
23. J. D. Vervoort, P. J. Patchett, *Geochim. Cosmochim. Acta* **60**, 3717 (1996).
24. D. G. Pearson, G. M. Nowell, *J. Petrol.* **45**, 439 (2004).
25. S. J. G. Galer, S. L. Goldstein, *Geochim. Cosmochim. Acta* **55**, 227 (1991).
26. E. B. Watson, T. M. Harrison, *Science* **308**, 841 (2005).
27. D. Trail, S. J. Mojzsis, T. M. Harrison, *Geochim. Cosmochim. Acta* **68**, A743 (2004).
28. R. Maas, P. D. Kinny, I. S. Williams, D. O. Froude, W. Compston, *Geochim. Cosmochim. Acta* **56**, 1281 (1992).
29. J. D. Vervoort, P. J. Patchett, J. Blichert-Toft, F. Albarede, *Earth Planet. Sci. Lett.* **168**, 79 (1999).
30. M. Boyet, R. W. Carlson, *Science* **309**, 576 (2005).
31. G. F. Davies, *Geochim. Cosmochim. Acta* **66**, 3125 (2002).
32. M. Boyet *et al.*, *Earth Planet. Sci. Lett.* **214**, 427 (2003).
33. G. Caro, B. Bourdon, J. L. Birck, S. Moorbath, *Nature* **423**, 428 (2003).

34. We thank M. McCulloch, P. Lanc, Z. Bruce, A. Schmitt, T. Ireland, and S. Mussett for their major contributions to this project. The work was supported at the Australian National University by Australian Research Council grant DP0342709 to T.M.H., by the French Institut National des Sciences de l'Univers and the Programme National de Planétologie grants to J.B.T. and F.A., and by NASA Exobiology grant NAG5-13497 to S.J.M.

Supporting Online Material
www.sciencemag.org/cgi/content/full/1117926/DC1
Materials and Methods
Figs. S1 and S2
Tables S1 to S3
References

25 July 2005; accepted 2 November 2005
Published online 17 November 2005;
10.1126/science.1117926
Include this information when citing this paper.

X-ray Structure of the EmrE Multidrug Transporter in Complex with a Substrate

Owen Pornillos, Yen-Ju Chen, Andy P. Chen, Geoffrey Chang*

EmrE is a prototype of the Small Multidrug Resistance family of efflux transporters and actively expels positively charged hydrophobic drugs across the inner membrane of *Escherichia coli*. Here, we report the x-ray crystal structure, at 3.7 angstrom resolution, of one conformational state of the EmrE transporter in complex with a translocation substrate, tetraphenylphosphonium. Two EmrE polypeptides form a homodimeric transporter that binds substrate at the dimerization interface. The two subunits have opposite orientations in the membrane and adopt slightly different folds, forming an asymmetric antiparallel dimer. This unusual architecture likely confers unidirectionality to transport by creating an asymmetric substrate translocation pathway. On the basis of available structural data, we propose a model for the proton-dependent drug efflux mechanism of EmrE.

A major obstacle to effective treatment of bacterial infections is the emergence of strains that are resistant to available antibiotics. Of particular concern are multidrug-resistant strains that cause common diseases such as tuberculosis, gonorrhea, and hospital-acquired staphylococcal infections (*1*). Multidrug resistance arises, in part, through the action of integral membrane proteins called multidrug transporters (*1*, *2*). Each of these transporters can actively expel a wide variety of drugs and toxic compounds from the cell. There are two broad classes of transporters: ATP-binding cassette (ABC) proteins directly couple drug efflux to adenosine 5′-triphosphate (ATP) hydrolysis, whereas secondary transporters use the energy derived from proton or cation electrochemical gradients across the lipid bilayer.

EmrE is a proton-dependent secondary transporter from *Escherichia coli* and is a prototype of the Small Multidrug Resistance (SMR) family (*3*, *4*). SMRs represent the smallest transporters in nature; each polypeptide has only 105 to 120 amino acid residues and four transmembrane helices, and forms homo- or heterooligomers (*3*). EmrE is well documented to function as a homooligomer (*5*–*9*) and confers resistance to positively charged hydrophobic antibiotics, such as tetracycline, ethidium, and tetraphenylphosphonium (TPP) (*3*, *4*). EmrE exchanges two or more protons per drug molecule through a "hydrophobic" translocation pathway (*10*, *11*).

The general model for multidrug efflux by EmrE and other secondary transporters is the alternating access mechanism (*12*, *13*). In this model, the EmrE transporter has at least two conformations, inward-facing and outward-facing, with the drug-binding site accessible to the cytoplasm or periplasm, respectively. Interconversion between the two conformations is promoted by drug and/or proton binding. Here, we describe the x-ray crystal structure of one conformation of the EmrE transporter in complex with the drug TPP. The structure was determined to 3.7 Å resolution by anomalous dispersion methods, using the arsonium analog of TPP and selenomethionine (SeMet)–substituted proteins (Fig. 1A) (*14*).

SeMet-labeled proteins used for this study were produced in a cell-free system, because SeMet-EmrE did not express well in vivo. Briefly, EmrE was expressed by use of the T7 promoter in *E. coli* lysates supplemented with nucleotide triphosphates, T7 polymerase, and appropriate amino acids (*14*). Experimental maps derived from Se and As data are very well correlated, indicating that in vitro– and in vivo–expressed EmrE proteins adopt a similar structure. Our work shows that cell-free methods are a viable alternative to traditional large-scale protein expression systems.

Consistent with biochemical studies showing that EmrE is primarily a dimer in detergent and binds drugs with a 2:1 protein/drug ratio (*9*, *15*), the asymmetric unit of the EmrE-TPP crystal is composed of two molecules of EmrE and one molecule of TPP (Fig. 1). The minimally functional unit of EmrE is therefore

Department of Molecular Biology, The Scripps Research Institute, 10550 North Torrey Pines Road, CB-105, La Jolla, CA 92037, USA.

*To whom correspondence should be addressed. E-mail: gchang@scripps.edu